

Large Misalignment between Stellar Bar and Dust Pattern in NGC 3488 Revealed by *Spitzer* and SDSS

C. Cao^{a,b,*} H. Wu^a Z. Wang^c L. C. Ho^d J. S. Huang^c
Z. G. Deng^{e,a}

^a*National Astronomical Observatories, Chinese Academy of Sciences, Beijing 100012, P. R. China*

^b*Graduate School of the Chinese Academy of Sciences, Beijing 100039, China*

^c*Harvard-Smithsonian Center for Astrophysics, 60 Garden Street, Cambridge, MA 02138*

^d*The Observatories of the Carnegie Institution of Washington, 813 Santa Barbara Street, Pasadena, CA 91101*

^e*College of Physical Sciences, Graduate School, Chinese Academy of Sciences, P.O. Box 3908, 100039 Beijing, China*

Abstract

A large position angle misalignment between the stellar bar and the distribution of dust in the late-type barred spiral NGC 3488 was discovered, using mid-infrared images from the *Spitzer Space Telescope* and optical images from the Sloan Digital Sky Survey (SDSS). The angle between the bar and dust patterns was measured to be $25^\circ \pm 2^\circ$, larger than most of the misalignments found previously in barred systems based on H α or H I/CO observations. The stellar bar is bright at optical and $3.6\mu\text{m}$, while the dust pattern is more prominent in the $8\mu\text{m}$ band but also shows up in the SDSS *u* and *g*-band images, suggesting a rich interstellar medium environment harboring ongoing star formation. This angular misalignment is unlikely to have been caused by spontaneous bar formation. We suggest that the stellar bar and the dust pattern may have different formation histories, and that the large misalignment was triggered by a tidal interaction with a small companion. A statistical analysis of a large sample of nearby galaxies with archival *Spitzer* data indicates that bar structure such as that seen in NGC 3488 is quite rare in the local Universe.

Key words: galaxies: individual(NGC 3488), galaxies: spiral, galaxies: structure, infrared: galaxies

PACS: 98.62.Hr

1 Introduction

Bar structure as a major non-axisymmetric feature on all scales is important in studying the morphology, mass and light distributions (e.g., Freeman 1996; Elmegreen & Elmegreen 1985; Elmegreen 1996; Elmegreen et al. 1996; Eskridge et al. 2000; Menéndez-Delmestre et al. 2007), star formation (e.g., Zurita et al. 2004; Knapen 2005; Ondrechen & van der Hulst 1983; Regan et al. 1996; Sheth et al. 2000), gas dynamics (e.g., Kormendy 1983; Bettoni & Galletta 1988; Sancisi et al. 1979; Benedict et al. 1996; Downes et al. 1996; Regan et al. 1999) and central activities (e.g., Ho et al. 1997b; Hawarden et al. 1986; Knapen et al. 2002; Sakamoto et al. 1999; Martini et al. 2003; Sheth et al. 2005) of disk galaxies. Theoretical models, including N-body and hydrodynamic simulations, generally confirm that bar formation is spontaneous and ubiquitous in disk evolution (e.g., Athanassoula 1992; Sellwood & Wilkinson 1993; Friedli & Benz 1993, 1995; Athanassoula & Bureau 1999). Because of the dissipative nature of the interstellar medium (ISM), the streaming motions of the molecular gas in and around bar regions can be different from the stellar orbits (Athanassoula 1992; Regan et al. 1999; Sheth et al. 2002). Due to the delayed star formation after the clouds have been triggered (~ 30 Myr; Vogel et al. 1988), the locations of gas/dust in galaxies can often be offset from that of young stars (e.g., Sheth et al. 2002; Phillips 1996; Martin & Friedli 1997). The molecular gas can be transported from galactic disk toward central region by the gravitational torques from bars (e.g., Sakamoto et al. 1999; Sheth et al. 2002, 2005), and the condensation of gas leads to subsequent circumnuclear star formation (e.g., Ho et al. 1997b; Knapen et al. 2002; Martini et al. 2003; Jogee et al. 2005; Fisher 2006).

Observationally, the gas/dust patterns can often be seen as dust lanes, atomic and molecular gas concentrations, or isophotes of H II regions with active star formation (Martin & Friedli 1997; Sakamoto et al. 1999; Regan et al. 1999; Rand et al. 1999; Crosthwaite et al. 2000; Sheth et al. 2002, 2005). As predicted by theoretical models (Athanassoula 1992; Friedli & Benz 1993, 1995), there is a small position angle misalignment between the gas/dust distribution and the stellar bar, usually of a few (and up to 10) degrees, in the sense that the former is *leading*. Kenney et al. (1991) found the gaseous pattern is offset from the major axis of the stellar distribution by $24^\circ \pm 6^\circ$ in M 101. Crosthwaite et al. (2000) found that the central gas distribution as indicated by H I map leads the stellar bar by almost 10° in the late-type galaxy IC 342. Similarly, Rozas et al. (2000) identified a large sample of H II regions in barred galaxy NGC 3359 and showed a position angle misalignment of a few degrees exists in H α and I-band images. They also pointed out that the *u*-band image of this galaxy

* Fax: 86-10-64873566

Email addresses: caochen@bao.ac.cn (C. Cao), hwu@bao.ac.cn (H. Wu).

shows a bar pattern more aligned with $H\alpha$, further suggesting massive star formation “at the leading edge of the bar”. Sheth et al. (2002) found offsets between molecular gas (CO) and star formation (traced by $H\alpha$) in bars of six nearby spirals, which were caused by the gas flow dependent star formation. Understanding the misalignment between stellar and gas/dust patterns and their formation scenarios is crucial for studying the ISM properties and star formation processes taking place in environments where gas dynamics are strongly perturbed (e.g., Regan et al. 1996; Martin & Friedli 1997; Sheth et al. 2000; Zurita et al. 2004), and also offers a good opportunity to study dynamical properties and secular evolution of barred galaxies (e.g., Kormendy 1983; Benedict et al. 1996; Regan et al. 1999; Kormendy & Kennicutt 2004; Sheth et al. 2005; Kormendy & Fisher 2005; Fisher 2006; Regan et al. 2006).

The *Spitzer Space Telescope*’s (Werner et al. 2004) observations in the mid-infrared, with its higher sensitivity and better angular resolution than previous observations (e.g., *ISO*), provide a new opportunity to study both stellar and gas/dust structures in galaxies (e.g., Pahre et al 2004; Wang et al. 2004; Cao & Wu 2007). In particular, the four Infrared Array Camera (IRAC; Fazio et al. 2004) bands from 3.6 to 8.0 μm probe both stellar continuum and warm dust emissions (of the so-called polycyclic aromatic hydrocarbon, or PAH, and dust continuum emissions) with identical spatial sampling, thus enabling a powerful probe to compare non-axisymmetric features such as bar structures involving gas/dust and stellar mass. Recently, *Spitzer* observations of nearby galaxies have demonstrated the importance of using mid-infrared images for studying galaxy secular evolution driven by bar instabilities (e.g., Fisher 2006; Regan et al. 2006).

In this paper, we present an analysis of data from *Spitzer* and SDSS of the late-type barred spiral galaxy NGC 3488. Previous studies show that, with an estimated distance of 39.9 Mpc (at this distance, 1'' corresponds to ~ 193 parsecs) and a total infrared luminosity of $L_{\text{TIR}} \approx 4.6 \times 10^9 L_{\odot}$ (Bell 2003), NGC 3488 [Hubble type SB(s)c] has a weak bar (~ 1.5 kpc), with spiral arms beginning at the bar’s end but without an inner ring. This is consistent with the conventional view that bars in most late-type spirals are relatively weak (Erwin 2005; Menéndez-Delmestre et al. 2007), and that weak bars tend to produce a SB(s) type response (in which the spiral arms begin at the ends of the bar; Kormendy & Kennicutt 2004). The data reduction is presented in §2, and results on the bar structures in NGC 3488 with multi-wavelengths analysis are described in §3. Possible explanations of the large misalignment between the bar and dust patterns are discussed in §4.

2 Data Reduction

Broad-band infrared images of NGC 3488 were acquired with IRAC on board *Spitzer*. The Basic Calibrated Data (BCD) were part of the Lockman Hole field in the *Spitzer* Wide-field Infrared Extragalactic (SWIRE) Survey (Lonsdale et al. 2003). Following the preliminary data reduction by the *Spitzer* Science Center pipeline, images of each of the four IRAC bands (3.6, 4.5, 5.8 and 8 μm) were mosaicked, after pointing refinement, distortion correction and cosmic-ray removal (Fazio et al. 2004; Huang et al. 2004; Wu et al. 2005; Surace et al. 2005; Cao & Wu 2007; Wen et al. 2007). The mosaicked images have pixel sizes of 0.6'' and angular resolutions (full width at half maximum, FWHM) of 1.9'', 2.0'', 1.9'' and 2.2'' for the four bands, respectively. The angular resolution of IRAC 8 μm images ($\sim 2.2''$) is significantly improved over that of pre-*Spitzer* data at similar wavelengths (e.g., $\sim 10''$ for ISOCAM LW2 at 7 μm ; Roussell et al. 2001).

In order to derive the dust-only 8 μm component (PAH and dust continuum emissions), we remove the stellar continuum from the IRAC 8 μm image by subtracting a scaled IRAC 3.6 μm image (assuming that the 3.6 μm emission is entirely due to old stellar population):

$$f_{\nu}(8\mu\text{m})_{\text{dust}} = f_{\nu}(8\mu\text{m}) - \eta_{8\mu\text{m}} f_{\nu}(3.6\mu\text{m}),$$

where the scaling factor $\eta_{8\mu\text{m}} = 0.232$ was calculated based on *Starburst99* synthesis model (Leitherer et al. 1999), assuming solar metallicity and a Salpeter initial mass function between 0.1 and 120 M_{\odot} . This approach has been adopted in several previous works (e.g., Helou et al. 2004; Wu et al. 2005; Regan et al. 2006; Bendo et al. 2006) for studying dust emissions and the 7.7 μm PAH feature based on broad-band measurements, and shown to be effective.

The five-band optical images (u, g, r, i, z) and the fiber spectrum for the central region (3'' diameter) of NGC 3488 were taken from the SDSS data archive (York et al. 2000; Stoughton et al. 2002). The background in each band was subtracted by fitting a low-order Legendre polynomial to it, after masking out all bright sources (Zheng et al. 1999; Wu et al. 2002). Figure 1 shows the three-color image of NGC 3488 derived from the SDSS data archive. North is up, and east is to the left, as denoted by the crosshair.

3 Results

3.1 Multi-wavelength View of Bar Structures in NGC 3488

The four-band IRAC images of NGC 3488 are shown in Figure 2. We find that NGC 3488 has two bar-like patterns that are bright in either stellar emission (at 3.6 and 4.5 μm) or warm dust emission (at 8 μm). We took the conventional approach of treating the bar as an elliptical feature for measuring its semi-major axis a and position angle PA. They can be measured with a fitting routine such as the `ellipse` task in IRAF. The PAs are approximately 36°, 36°, 20°, 15° for the bars in the 3.6, 4.5, 5.8, 8 μm band, respectively. Uncertainties of the position angles are estimated to be $\pm 2^\circ$, derived from the deviation of PAs along the major axis of the bar. Taking the mean of the two shorter wavelength bands as representing the stellar bar, we measured that it trails the dust pattern traced primarily by the continuum-subtracted 8 μm emission (Fig. 3c), by a large position angle difference. Spiral arms with bright knots are also visible in the 8 μm image: they appear to begin at the end of the dust pattern (Fig. 3d).

For the SDSS images, the PA of the bar was also measured using `ellipse`. The PA of the optical bar measured in this way is nearly identical ($\sim 40^\circ$) in the SDSS g , r , i , z -band images, and is also spatially coincident, within the measurement uncertainty of $\sim \pm 2^\circ$, with that of the IRAC 3.6 and 4.5 μm images, but trails the dust pattern at 8 μm by 25° (Fig. 3b). However, the bar in the SDSS u -band is quite different from that in the other SDSS bands: at PA $\approx 15^\circ$, it is instead much better aligned with the dust pattern bright at IRAC 8 μm (Fig. 3a).

The deprojected values of the relative length [$L_b(i)$] and the misalignment between the stellar bar and the dust pattern [$\theta(i)$] are calculated using the equations given by Martin (1995):

$$L_b(i) = \frac{2a[\cos^2(\phi_a) + \sec^2(i)\sin^2(\phi_a)]^{1/2}}{D_{25}}$$

$$\theta(i) = \arctan[\cos(i)\tan(\phi_{a,8\mu\text{m}})] - \arctan[\cos(i)\tan(\phi_{a,\text{stellar}})],$$

where i is the inclination angle of NGC 3488 ($\sim 49.5^\circ$, calculated using the formula given by Bottinelli et al. 1983), a is the length of the semi-major axis, ϕ_a is the angle between the patterns (dust or stellar) and the node lines (the major axis defines the PA of the galaxy, $\sim 175^\circ$), and D_{25} is the diameter of NGC 3488 at a B -band surface brightness of 25 mag arcsec $^{-2}$ (~ 1.86 arcmin).

¹ These parameters of the patterns are summarized in Table 1. The angular misalignment between the optical bar and the infrared dust pattern, $\theta(i)$, is approximately 20° after correcting for inclination effect. Uncertainties of these parameters can be as large as 20%, due mostly to simplistic assumptions concerning projection effects and the difficulty in decoupling the bar from the bulge (Martin 1995; Martin & Friedli 1997), especially in the IRAC $8\mu\text{m}$ image. Nevertheless, this angular misalignment, assuming it represents the misalignment between the dust and stellar patterns, belongs to one of the largest misalignments found in previous observations or in typical numerical simulations.

Besides the bright stellar bar, a faint and clumpy bar-like structure appears to be present in the SDSS g -band image (Fig. 4, left panel). We use two different techniques to enhance the visibility of this structure: unsharp masking (e.g., Walterbos et al. 1994) and deconvolution (Fig. 4, right panel). Unsharp masking was made by using a 2-pixel wide (2σ) Gaussian filter. The deconvolution was performed with the task `lucy` (Lucy 1974) in IRAF, using a point-spread function derived from the associated psField file of the SDSS data; the total number of iterations is 30. The PA of this faint bar-like structure is approximately $15^\circ \pm 2^\circ$, so it is spatially coincident with the patterns in u -band and $8\mu\text{m}$ images.

3.2 Stellar Populations in Bars

The bar bright at optical (SDSS) and IRAC 3.6, $4.5\mu\text{m}$ is known to be dominated by old stellar population. Gadotti & de Souza (2006) showed that the bar color index can be used as an indicator of the bar age: old bars are on average redder than young ones. The SDSS $g-r$ and $g-i$ colors of the stellar bar of NGC 3488 were compared with an instantaneous burst model calculated based on GALAXEV (Bruzual & Charlot 2003), adopting a Salpeter initial mass function and solar metallicity as initial conditions. This comparison shows that the stellar bar bright in optical and IRAC 3.6 and $4.5\mu\text{m}$ bands is evolved, with a mean age of the order of 4 Gyr.

The pattern bright at $8\mu\text{m}$ is dominated by the strong $7.7\mu\text{m}$ PAH feature and warm dust continuum emission from very small grains, while the pattern shown in the IRAC $5.8\mu\text{m}$ image is probably a mixture of stellar and dust ($6.2\mu\text{m}$ PAH and warm dust) components. From the correlation between $8\mu\text{m}$ dust emission and star formation activities (Wu et al. 2005; Calzetti et al. 2005) and the previous result that $8\mu\text{m}$ dust and $24\mu\text{m}$ hot dust emission are

¹ The PA, D_{25} , and R_{25} of NGC 3488 were taken from The Third Reference Catalogue of Bright Galaxies (de Vaucouleurs et al. 1991).

well correlated on kiloparsec scales ² (e.g., Bendo et al. 2006), we suggest that the dust pattern seen at $8\mu\text{m}$ is associated with young stars and thus represents recent star forming activity. Some authors (e.g., Regan et al. 2006; R. C. Kennicutt, priv. comm.), however, argue that PAH emission is likely a better tracer of the general ISM rather than star-forming regions heated by young, massive stars. The coincidence of the bar shown in the u -band with that bright at $8\mu\text{m}$ (Fig. 3a) confirms that there exists a young stellar population in the region of the dust pattern.

3.3 Star Formation Rates

The star formation rate (SFR) in the bar region of NGC 3488 can be estimated using either the $\text{H}\alpha$ line flux or the $8\mu\text{m}$ dust emission. The SDSS spectrum, taken through a $3''$ -diameter (~ 0.58 kpc) fiber, indicates that the central region can be classified as an “H II nucleus” (Ho et al. 1997a), one whose main source of ionizing photons derives from young stars. The $\text{H}\alpha$ -based SFR is calculated using Equation B3 of Hopkins et al. (2003), after correcting for extinction using the observed Balmer decrement (Calzetti 2001):

$$SFR_{\text{H}\alpha}(M_{\odot}\text{yr}^{-1}) = 4\pi D_1^2 S_{\text{H}\alpha} \left(\frac{S_{\text{H}\alpha}/S_{\text{H}\beta}}{2.86} \right)^{2.114} \frac{1}{1.27 \times 10^{34}},$$

where $S_{\text{H}\alpha}$ and $S_{\text{H}\beta}$ are the stellar absorption-corrected line fluxes, derived from the emission-line catalog given by MPA-SDSS (Tremonti et al. 2004). The measured SFR for the central $3''$ based on $\text{H}\alpha$ is $0.0077 M_{\odot} \text{yr}^{-1}$.

To estimate the SFR along the bar, we use the $8\mu\text{m}$ dust emission, which is thought to be measure of the SFR in galaxies (Wu et al. 2005). From Equation 4 of Wu et al. (2005):

$$SFR_{8\mu\text{m dust}}(M_{\odot}\text{yr}^{-1}) = \frac{\nu L_{\nu}(8\mu\text{m dust})}{1.57 \times 10^9 L_{\odot}}.$$

An aperture of $3''$ diameter was selected for measuring the SFR centered on the nucleus using the dust-only $8\mu\text{m}$ image, to enable a sensible comparison with the SFR derived from the $\text{H}\alpha$ flux. The SFR measured in this way is $0.0079 M_{\odot} \text{yr}^{-1}$, consistent with that derived from $\text{H}\alpha$. This result indicates that the $8\mu\text{m}$ dust emission can be used as a tracer of the SFR in the central region of galaxies, at least for the case of NGC 3488. The enhanced $8\mu\text{m}$ emission in the

² MIPS $24\mu\text{m}$ emission, which is mainly due to hot dust emission from very small grains, is thought to be a good measure of the SFR in galaxies (e.g., Wu et al. 2005; Calzetti et al. 2005; Pérez-González et al. 2006).

central region of NGC 3488 is consistent with the result that barred galaxies tend to have strong central excesses in $8\mu\text{m}$ emission (Regan et al. 2006), which suggests that bars induce gas inflows toward the center of galaxies as an internal process of galaxy secular evolution (e.g., Sakamoto et al. 1999; Sheth et al. 2000, 2002, 2005; Jogee et al. 2005). We also estimated the total SFR along the bar after excluding the contribution from the central region. The photometry was performed on the dust-only $8\mu\text{m}$ image using an ellipse with a semi-major axis of $3''$ and an ellipticity of 0.5, chosen to match the isocontour of the dust pattern. The measured SFR for the bar and nucleus is $\sim 0.0150 M_{\odot} \text{ yr}^{-1}$, which implies that the SFR along the bar is roughly $0.0072 M_{\odot} \text{ yr}^{-1}$, comparable to the value at the nucleus.

4 Discussion

4.1 Possible Formation Scenarios of the Misalignment Between Bars in NGC 3488

Martin & Friedli (1997) found that the $\text{H}\alpha$ bars (tracing young stars and H II regions) and stellar bars are misaligned by up to 10° among 11 barred galaxies. Friedli & Benz (1993, 1995), using their N-body + SPH simulations of spontaneous bar formation, showed that the H II regions tend to lead the stellar bar by an angle of several degrees. In these simulations the misalignments between bars are similar to those observed, and they occur as a result of orbit crossings of gas motion, mostly at early epochs during the formation of a strong, fast-rotating bar in the absence of an inner Lindblad resonance (Martin & Friedli 1997). The best example is NGC 3359, in which star formation is completely absent in the galaxy nucleus (Martin & Friedli 1997), and the age of the bar is young (~ 400 Myr; Martin & Roy 1995). But this is unlikely to be the case in NGC 3488, due to the fact that the age of its stellar bar (~ 4 Gyr) is much older than bars in the spontaneous bar formation scenario (e.g., NGC 3359).

Alternatively, perhaps the morphology of this galaxy represents an episode shortly after the capture of a small, secondary galaxy. In such a galaxy merger scenario, the stellar and dust patterns may have different formation histories. The stellar bar may have formed previously as in a spontaneous formation scenario, and the dust pattern could be tidally induced later from a dwarf galaxy swallowed by NGC 3488. The different stellar populations in the stellar bar and the dust pattern (see §3.2) also support this scenario. Berentzen et al. (2003) investigated the dynamical effects of the interaction between an initially barred galaxy and a small companion, using N-body/SPH numerical simulations. They found that the interactions can produce offset bars, nuclear

and circumnuclear disks, and tidal arms connected to the end of the bar. Based on their results that the fate of the stellar bar is determined by the impact position, we speculate that in NGC 3488 there may have been an impact on the bar major axis when the bar was weak. In such a case, the tidal force exerted on the bar does not disrupt much the bar structure (i.e., the stellar bar survived after the impact). The nearby bright, compact object toward the northeast of the SDSS images (see Fig. 3b), identified as SDSS J110124.04+574045.1, is a plausible candidate for a dwarf galaxy that may have hit NGC 3488. Its colors are very blue ($u - g = 0.309$, $g - r = -0.222$, $r - i = -0.757$) and similar to those of irregular galaxies (Fukugita et al. 1995). And its absolute magnitude (-12.73 , -13.59 , -13.93 , -13.82 , -13.81 for u , g , r , i , z , respectively) are located at the faint end of the luminosity function of extremely low-luminosity galaxies (Blanton et al. 2005), if we assume that its distance is the same as that of NGC 3488 (39.9 Mpc). However, we cannot exclude the possibility that it is a foreground white dwarf star superposed on NGC 3488, since its very blue colors are consistent with those of spectroscopically identified white dwarf stars in SDSS (Kleinman et al. 2004).

4.2 Frequency of Large Misalignments Between Bars Among Galaxies Revealed By *Spitzer*

Large misalignments ($>10^\circ$) between stellar bars (bright at optical and $3.6\mu\text{m}$) and dust distributions (shown at $8\mu\text{m}$) are quite rare among nearby barred galaxies with archival *Spitzer* data. We have examined ~ 50 barred spirals (SB and SAB) in the *Spitzer* Infrared Nearby Galaxies Survey (SINGS, Kennicutt et al. 2003) and in the Mid-IR Hubble Atlas of Galaxies (a *Spitzer* GTO program, PID: #69, PI: G. Fazio; see also Pahre et al. 2004), and found that *none* of them shows a misalignment as large as that found in NGC 3488. Most of the galaxies only have a single old stellar bar, which is bright at IRAC 3.6 and $4.5\mu\text{m}$ but absent at $8\mu\text{m}$ (e.g., NGC 7080). Others that have younger bars always show good alignment between 3.6 and $8\mu\text{m}$ (e.g., NGC 7479, consistent with the previous result that no misalignment was observed between its $\text{H}\alpha$ and stellar bars; Martin & Friedli 1997). This statistical evidence indicates that the bar structure seen in NGC 3488 is quite rare among barred galaxies in the local Universe, and that the misalignment between bar and dust patterns may be a short-lived phenomenon in the evolutionary history of the galaxy. However, any firm conclusion must await a quantitative analysis of a large, well-defined, and unbiased sample of barred galaxies.

5 Summary

Using mid-infrared images from *Spitzer* and optical images from SDSS, we show that the late-type barred spiral galaxy NGC 3488 contains two misaligned patterns, one composed of old stars and the other young stars and dust. The angle between the two patterns ($\sim 25^\circ$) is among the largest ever reported. The stellar bar is bright in the optical and in the IRAC 3.6 and $4.5\mu\text{m}$ bands, and is dominated by old stars. The dust pattern is more prominent in the $8\mu\text{m}$ band, but also shows up in the SDSS *u* and *g* bands; it traces regions of recent or ongoing star formation. The dust pattern could be tidally induced by a dwarf galaxy swallowed by NGC 3488. From examination of mid-infrared images of a large sample of nearby barred galaxies with archival *Spitzer* data, we find that bar structure such as that found in NGC 3488 is quite rare in the local Universe.

To further test the hypothesis that the large misalignment in NGC 3488 was triggered by a recent merger, it would be desirable to obtain deeper imaging observations of the system in order to search for morphological features suggestive of tidal interactions. Obtaining a spectrum of the candidate dwarf galaxy would help validate its physical association with NGC 3488. Additional numerical simulations will help to validate whether two large-scale patterns can coexist over long time scales, since it is possible that the competing torques will introduce chaos to the system (I. Berentzen, priv. comm.).

Acknowledgments

We would like to thank the anonymous referee for very constructive comments and suggestions. We thank X.-Y. Xia, S. Mao, R. Kennicutt, I. Berentzen for advice and helpful discussions, and C.-N. Hao, J.-L. Wang, F.-S. Liu for their capable assistance throughout the process of *Spitzer* data reductions. This project is supported by NSFC No.10273012, No.10333060, No.10473013, No.10373008. This work is based in part on observations made with the *Spitzer Space Telescope*, which is operated by the Jet Propulsion Laboratory, California Institute of Technology under NASA contract 1407. Funding for the SDSS and SDSS-II has been provided by the Alfred P. Sloan Foundation, the Participating Institutions, the National Science Foundation, the U.S. Department of Energy, the National Aeronautics and Space Administration, the Japanese Monbukagakusho, the Max Planck Society, and the Higher Education Funding Council for England. The SDSS Web Site is <http://www.sdss.org/>. The SDSS is managed by the Astrophysical Research Consortium for the Participating Institutions. The Participating Institutions are the American Museum of Natural History, Astrophysical Institute Potsdam, University of Basel, Cambridge University, Case Western Reserve University, University of Chicago, Drexel Uni-

versity, Fermilab, the Institute for Advanced Study, the Japan Participation Group, Johns Hopkins University, the Joint Institute for Nuclear Astrophysics, the Kavli Institute for Particle Astrophysics and Cosmology, the Korean Scientist Group, the Chinese Academy of Sciences (LAMOST), Los Alamos National Laboratory, the Max-Planck-Institute for Astronomy (MPIA), the Max-Planck-Institute for Astrophysics (MPA), New Mexico State University, Ohio State University, University of Pittsburgh, University of Portsmouth, Princeton University, the United States Naval Observatory, and the University of Washington.

References

- Athanassoula, E. 1992, *MNRAS*, 259, 328
Athanassoula, E., & Bureau, M. 1999, *ApJ*, 522, 699
Bell, E. F. 2003, *ApJ*, 586, 794
Bendo, G. J., et al. 2006, *ApJ*, 652, 283
Benedict, F. G., Smith, B. J., & Kenney, J. D. P. 1996, *AJ*, 111, 1861
Berentzen, I., Athanassoula, E., Heller, C. H., & Fricke, K. J. 2003, *MNRAS*, 341, 343
Bettoni, D., & Galletta, G. 1988, *A&A*, 190, 52
Blanton, M. R., Lupton, R. H., Schlegel, D. J., Strauss, M. A., Brinkmann, J., Fukugita, M., & Loveday, J. 2005, *ApJ*, 631, 208
Bottinelli, L., Gouguenheim, L., Paturel, G., & de Vaucouleurs, G. 1983, *A&A*, 118, 4
Bruzual, G., & Charlot, S. 2003, *MNRAS*, 344, 1000
Calzetti, D. 2001, *PASP*, 113, 1449
Calzetti, D., et al. 2005, *ApJ*, 633, 871
Cao, C., & Wu, H. 2007, *AJ*, 133, 1710
Crosthwaite, L. P., Turner, J. L., & Ho, P. T. P. 2000, *AJ*, 119, 1720
Downes, D., Reynaud, D., Solomon, P. M., & Radford, S. J. E. 1996, *ApJ*, 461, 186
de Vaucouleurs, G., de Vaucouleurs, A., Corwin, H. G., Buta, R. J., Paturel, G. & Fouque, P. 1991, *Third Reference Catalogue of Bright Galaxies* (New York: Springer)
Elmegreen, B. G., & Elmegreen, D. M. 1985, *ApJ*, 288, 438
Elmegreen, D. M. 1996, *IAU Colloq. 157: Barred Galaxies*, 91, 23
Elmegreen, B. G., Elmegreen, D. M., Chromey, F. R., Hasselbacher, D. A., & Bissell, B. A. 1996, *AJ*, 111, 2233
Erwin, P. 2005, *MNRAS*, 364, 283
Eskridge, P. B., et al. 2000, *AJ*, 119, 536
Fazio, G. G., et al. 2004, *ApJS*, 154, 10
Fisher, D. B. 2006, *ApJl*, 642, L17
Freeman, K. C. 1996, *IAU Colloq. 157: Barred Galaxies*, 91, 1

Friedli, D., & Benz, W. 1993, *A&A*, 268, 65
 Friedli, D., & Benz, W. 1995, *A&A*, 301, 649
 Fukugita, M., Shimasaku, K., & Ichikawa, T. 1995, *PASP*, 107, 945
 Gadotti, D. A., & de Souza, R. E. 2006, *ApJS*, 163, 270
 Hawarden, T. G., Mountain, C. M., Leggett, S. K., & Puxley, P. J. 1986,
MNRAS, 221, 41P
 Helou, G., et al. 2004, *ApJS*, 154, 253
 Ho, L. C., Filippenko, A. V., & Sargent, W. L. W. 1997a, *ApJ*, 487, 579
 Ho, L. C., Filippenko, A. V., & Sargent, W. L. W. 1997b, *ApJ*, 487, 591
 Hopkins, A. M., et al. 2003, *ApJ*, 599, 971
 Huang, J.-S., et al. 2004, *ApJS*, 154, 44
 Jogee, S., Scoville, N., & Kenney, J. D. P. 2005, *ApJ*, 630, 837
 Kenney, J. D. P., Scoville, N. Z., & Wilson, C. D. 1991, *ApJ*, 366, 432
 Kennicutt, R. C., et al. 2003, *PASP*, 115, 928
 Kleinman, S. J., et al. 2004, *ApJ*, 607, 426
 Knapen, J. H., Pérez-Ramírez, D., & Laine, S. 2002, *MNRAS*, 337, 808
 Knapen, J. H. 2005, *Astronomy and Geophysics*, 46, 28
 Kormendy, J. 1983, *ApJ*, 275, 529
 Kormendy, J., & Kennicutt, R. C. 2004, *ARA&A*, 42, 603
 Kormendy, J., & Fisher, D. B. 2005, *Revista Mexicana de Astronomia y Astrofisica Conference Series*, 23, 101
 Leitherer, C., et al. 1999, *ApJS*, 123, 3
 Lonsdale, C. J., et al. 2003, *PASP*, 115, 897
 Lucy, L. B. 1974, *AJ*, 79, 745
 Martin, P. 1995, *AJ*, 109, 2428
 Martin, P., & Friedli, D. 1997, *A&A*, 326, 449
 Martin, P., & Roy, J.-R. 1995, *ApJ*, 445, 161
 Martini, P., Regan, M. W., Mulchaey, J. S., & Pogge, R. W. 2003, *ApJ*, 589,
 774
 Menéndez-Delmestre, K., Sheth, K., Schinnerer, E., Jarrett, T. H., & Scoville,
 N. Z. 2007, *ApJ*, 657, 790
 Ondrechen, M. P., & van der Hulst, J. M. 1983, *ApJ*, 269, L47
 Pahre, M. A., Ashby, M. L. N., Fazio, G. G., & Willner, S. P. 2004, *ApJS*,
 154, 235
 Pérez-González, P. G., et al. 2006, *ApJ*, 648, 987
 Phillips, A. C. 1996, *IAU Colloq. 157: Barred Galaxies*, 91, 44
 Rand, R. J., Lord, S. D., & Higdon, J. L. 1999, *ApJ*, 513, 720
 Regan, M. W., Teuben, P. J., Vogel, S. N., & van der Hulst, T. 1996, *AJ*, 112,
 2549
 Regan, M. W., Sheth, K., & Vogel, S. N. 1999, *ApJ*, 526, 97
 Regan, M. W., et al. 2006, *ApJ*, 652, 1112
 Roussel, H., et al. 2001, *A&A*, 369, 473
 Rozas, M., Zurita, A., & Beckman, J. E. 2000, *A&A*, 354, 823
 Sakamoto, K., Okumura, S. K., Ishizuki, S., & Scoville, N. Z. 1999, *ApJ*, 525,
 691

- Sancisi, R., Allen, R. J., & Sullivan, W. T., III 1979, *A&A*, 78, 217
- Sellwood, J. A., & Wilkinson, A. 1993, *Reports of Progress in Physics*, 56, 173
- Sheth, K., Regan, M. W., Vogel, S. N., & Teuben, P. J. 2000, *ApJ*, 532, 221
- Sheth, K., Vogel, S. N., Regan, M. W., Teuben, P. J., Harris, A. I., & Thornley, M. D. 2002, *AJ*, 124, 2581
- Sheth, K., Vogel, S. N., Regan, M. W., Thornley, M. D., & Teuben, P. J. 2005, *ApJ*, 632, 217
- Stoughton, C., et al. 2002, *AJ*, 123, 485
- Surace, J. A., et al. 2005, 'The SWIRE Data Release 2: Image Atlases and Source Catalogs for ELAIS-N1, ELAIS-N2, XMM-LSS, and the Lockman Hole'
- Vogel, S. N., Kulkarni, S. R., & Scoville, N. Z. 1988, *Nature*, 334, 402
- Walterbos, R. A. M., Braun, R., & Kennicutt, R. C., Jr. 1994, *AJ*, 107, 184
- Wang, Z., et al. 2004, *ApJS*, 154, 193
- Wen, X.-Q., Wu, H., Cao, C., & Xia, X.-Y. 2007, *Chinese Journal of Astronomy and Astrophysics*, 7, 187
- Werner, M. W., et al. 2004, *ApJS*, 154, 1
- Wu, H., et al. 2002, *AJ*, 123, 1364
- Wu, H., Cao, C., Hao, C.-N., Liu, F.-S., Wang, J.-L., Xia, X.-Y., Deng, Z.-G., & Young, C. K.-S. 2005, *ApJ*, 632, L79
- York, D. G., et al. 2000, *AJ*, 120, 1579
- Zheng, Z., et al. 1999, *AJ*, 117, 2757
- Zurita, A., Relaño, M., Beckman, J. E., & Knapen, J. H. 2004, *A&A*, 413, 73

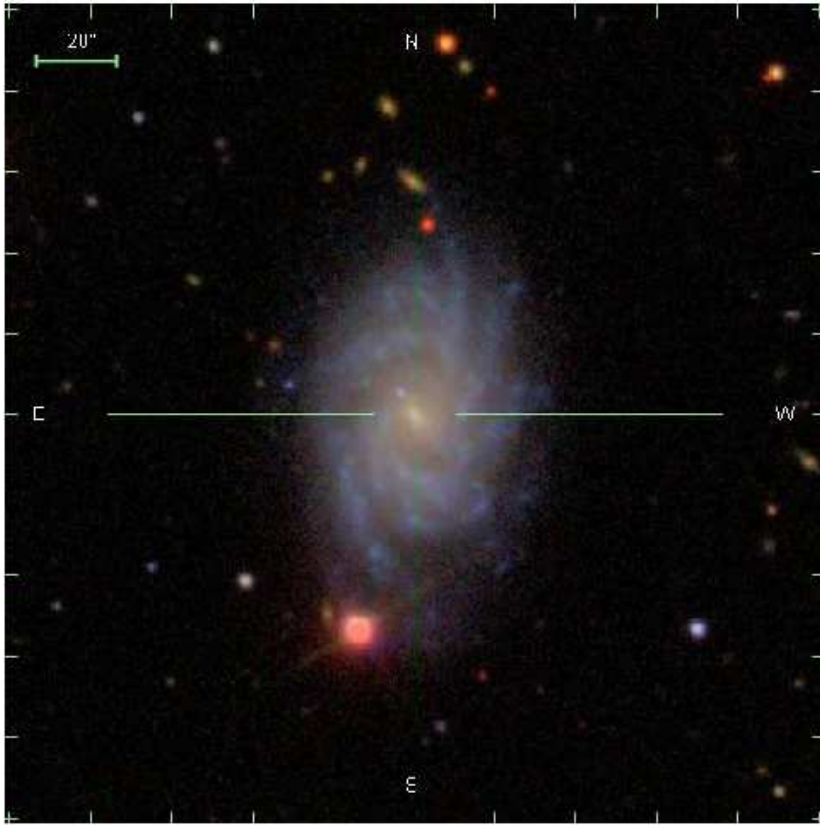


Fig. 1. Three-color image of NGC 3488 derived from the SDSS data archive. North is up, and east is to the left, as denoted by the crosshair.

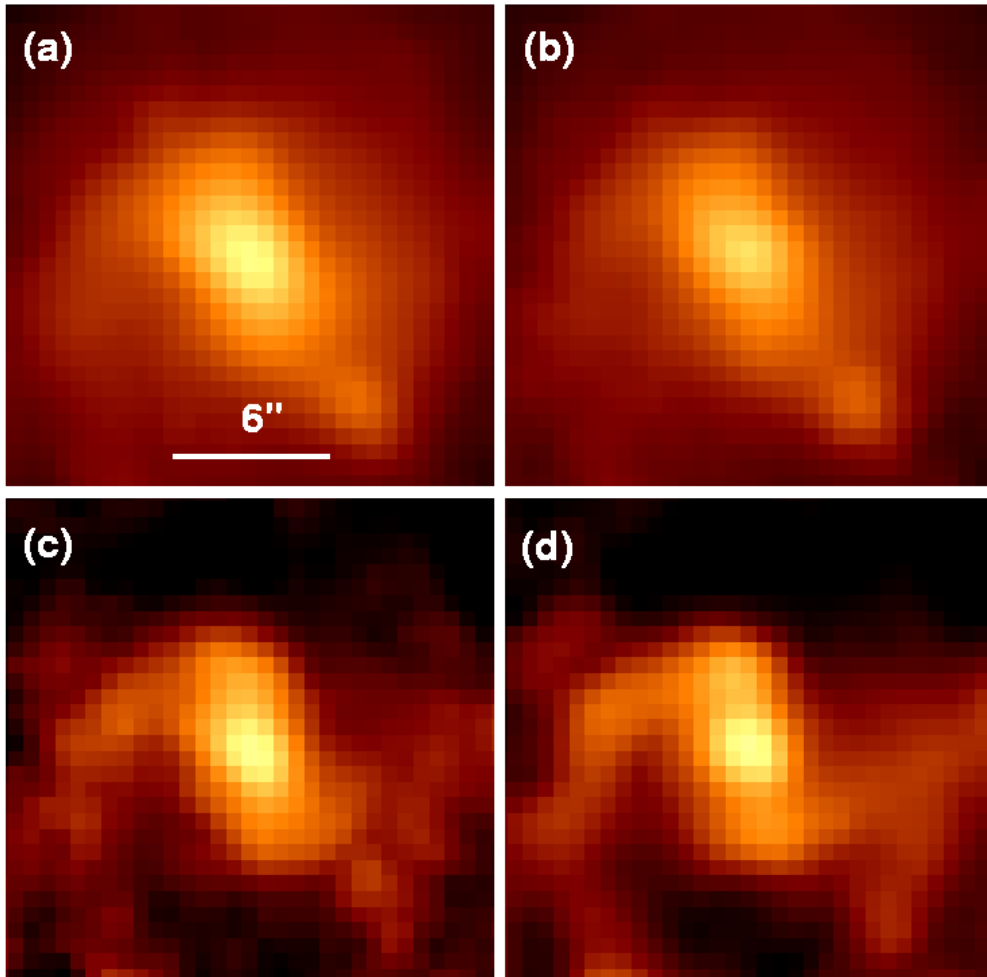


Fig. 2. The *Spitzer* IRAC four-band images [from (a) to (d): 3.6, 4.5, 5.8, 8 μ m] of the bar region in NGC 3488. North is up; East is to the left. The stellar bar bright at 3.6 and 4.5 μ m and the dust pattern bright at 8 μ m are misaligned by a large angle.

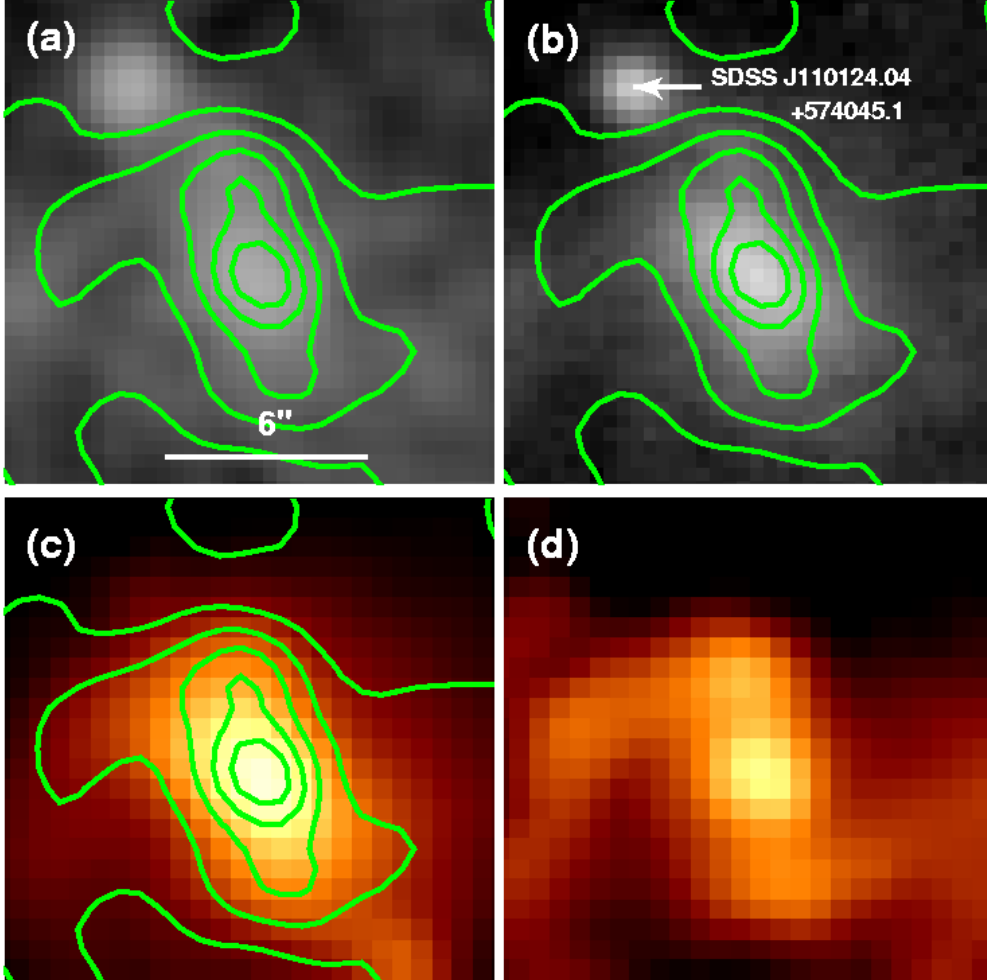


Fig. 3. From (a) to (d): the SDSS u -band, g -band, IRAC $3.6\mu\text{m}$, and dust-only $8\mu\text{m}$ images of the bar region in NGC 3488. North is up; East is to the left. The u -band image was smoothed using a 2-pixel wide (2σ) Gaussian filter. Contours of the dust-only $8\mu\text{m}$ image are superposed on the u -band, g -band, and IRAC $3.6\mu\text{m}$ images. A large misalignment by an apparent angle (θ) of about 25° is shown between the bright bar at optical (with a PA of $\sim 40^\circ$) and the dust distribution shown in the dust-only $8\mu\text{m}$ image (with a PA of $\sim 15^\circ$). A nearby compact, bright object (SDSS J110124.04+574045.1) is shown in the northeast of the SDSS images.

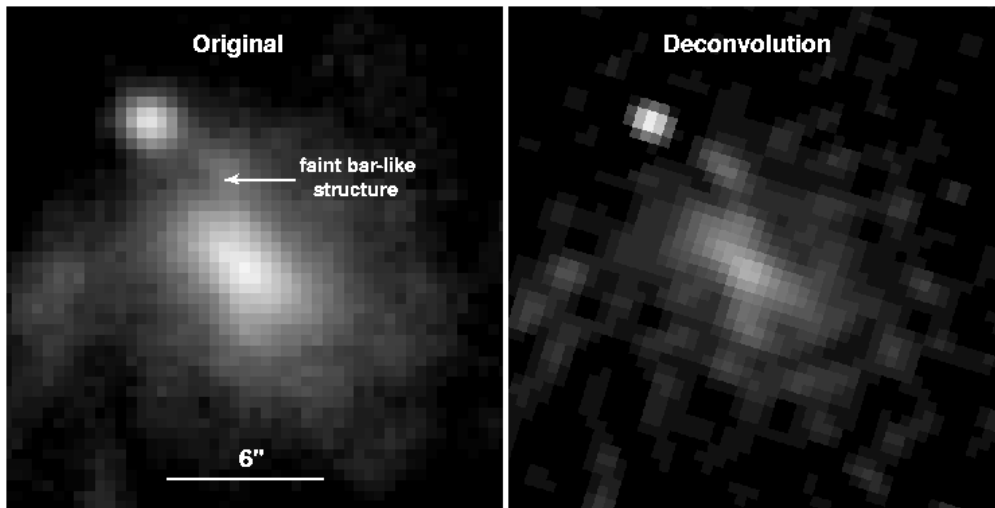


Fig. 4. The original (left) and deconvolved (right) SDSS g -band images of the bar region in NGC 3488. North is up; East is to the left. A faint and clumpy bar-like structure is suggested in the deconvolved images.

Table 1
 Properties of bar and dust patterns

Regions	a ["]	$L_b(i)$	PA[°]	θ [°]	$\theta(i)$ [°]	Image
	(1)	(2)	(3)	(4)	(5)	(6)
Stellar Bar	4.2	0.111	40.0			SDSS g band
				25.0	19.7	
Dust Pattern	3.0	0.067	15.0			IRAC $8\mu\text{m}$

Notes.—Col.(1): The lengths of semi-major axis of the stellar bar and dust pattern; Col.(2): The relative lengths of the patterns; Col.(3): Position angles measured in the conventional manner, from North through East; Col.(4): The measured angular misalignment between stellar and dust patterns; Col.(5): The angular misalignment after correcting for inclination effect; Col.(6): Images used for the measurements.